

Towards a Near Infrared Spectroscopy-Based Estimation of Operator Attentional State

G rard Derosi re^{1,2*}, Sami Dalhoumi^{2,3}, St phane Perrey¹, G rard Dray³, Tomas Ward²

1 Movement to Health (M2H), EuroMov, Montpellier-1 University, Montpellier, France, **2** Biomedical Engineering Research Group (BERG), National University of Ireland Maynooth (NUIM), Maynooth, Ireland, **3** Laboratoire de G nie Informatique et d'Ing nierie de Production (LG2IP), Ecole des Mines d'Al s, Nimes, France

Abstract

Given the critical risks to public health and safety that can involve lapses in attention (e.g., through implication in workplace accidents), researchers have sought to develop cognitive-state tracking technologies, capable of alerting individuals engaged in cognitively demanding tasks of potentially dangerous decrements in their levels of attention. The purpose of the present study was to address this issue through an investigation of the reliability of optical measures of cortical correlates of attention in conjunction with machine learning techniques to distinguish between states of full attention and states characterized by reduced attention capacity during a sustained attention task. Seven subjects engaged in a 30 minutes duration sustained attention reaction time task with near infrared spectroscopy (NIRS) monitoring over the prefrontal and the right parietal areas. NIRS signals from the first 10 minutes of the task were considered as characterizing the 'full attention' class, while the NIRS signals from the last 10 minutes of the task were considered as characterizing the 'attention decrement' class. A two-class support vector machine algorithm was exploited to distinguish between the two levels of attention using appropriate NIRS-derived signal features. Attention decrement occurred during the task as revealed by the significant increase in reaction time in the last 10 compared to the first 10 minutes of the task ($p < .05$). The results demonstrate relatively good classification accuracy, ranging from 65 to 90%. The highest classification accuracy results were obtained when exploiting the oxyhemoglobin signals (i.e., from 77 to 89%, depending on the cortical area considered) rather than the deoxyhemoglobin signals (i.e., from 65 to 66%). Moreover, the classification accuracy increased to 90% when using signals from the right parietal area rather than from the prefrontal cortex. The results support the feasibility of developing cognitive tracking technologies using NIRS and machine learning techniques.

Citation: Derosi re G, Dalhoumi S, Perrey S, Dray G, Ward T (2014) Towards a Near Infrared Spectroscopy-Based Estimation of Operator Attentional State. *PLoS ONE* 9(3): e92045. doi:10.1371/journal.pone.0092045

Editor: Yoko Hoshi, Tokyo Metropolitan Institute of Medical Science, Japan

Received: November 6, 2013; **Accepted:** February 19, 2014; **Published:** March 14, 2014

Copyright:   2014 Derosi re et al. This is an open-access article distributed under the terms of the Creative Commons Attribution License, which permits unrestricted use, distribution, and reproduction in any medium, provided the original author and source are credited.

Funding: This work was supported by the LabEx "Numerisation and Modelisation for Health and Environment" (ANR-10-LABX-20-01) and the French University Institute (IUF-UM1 1195-UM2 110744). The funders had no role in study design, data collection and analysis, decision to publish, or preparation of the manuscript.

Competing Interests: The authors have declared that no competing interests exist.

* E-mail: gerard.derosiere@univ-montp1.fr

Introduction

Attention to a cognitively demanding task cannot be maintained at a high level indefinitely. During a sustained attention task, as time elapses, the level of attention progressively diminishes negatively impacting task performance [1]. Lapses in attention are behaviorally characterized by an increase in reaction time (RT; e.g., [2]) a phenomenon that can impact severely on activities of daily living. For instance, work-related injuries [3,4] and traffic accidents [5] are typical consequences of attention decrement. Recently, researchers have sought to develop cognitive tracking technologies capable of alerting users to such degradation in their attention levels [6,7]. The aspiration is that such technology can facilitate optimal human-machine interactions in real-life settings, both in the workplace and in the home.

While several indicators have been suggested for the detection of task-related changes in attention levels such as blink duration and rate [8], heart rate variability [9] and electroencephalographic measures [6] there is, however, no accepted "gold standard" technology for detecting attention decrement [7], aside from RT measures. Although some authors suggest that EEG-measured changes in brain activity might represent the most promising indicator of attention decrement [5], other studies have proposed

that hybrid systems - based on the multimodal fusion of a number of indicators - may allow for more robust performance [10,11]. In this vein, optical neuroimaging, namely Near Infrared Spectroscopy (NIRS), may represent a viable additional and complementary method for cognitive state monitoring. The purpose of this study is to address the issue by investigating the capability of this increasingly exploited neuroimaging method (i.e., NIRS), to detect real-time changes in brain activity related to decrements in the level of attention during a sustained attention task. In particular, this study investigates the sensitivity of (i) different NIRS-measured hemodynamic variables as well as (ii) different attention-related cortical areas to the attention decrement phenomenon.

NIRS is a versatile neuroimaging tool increasingly adopted in the neuroimaging-community [12,13]. Ayaz *et al.* [14] assert that "NIRS is safe, highly portable, user-friendly and relatively inexpensive, with rapid application times and near-zero run-time costs" [15–19]. The modality has potential, as a portable measurement system for cognitive state monitoring outside the laboratory environment [20,21]. Functional NIRS utilizes, as fMRI does, the tight coupling between neuronal activity and regional cerebral blood flow [22] to infer brain activation state from changes in oxy- (O_2Hb) and deoxy-hemoglobin (HHb) concentrations characterizing the cortical hemodynamic response. Recently NIRS-derived cortical

hemodynamic responses have been demonstrated to be sensitive to attention decrement during sustained attention tasks [23–30]. Further, it has been demonstrated through machine learning studies based on NIRS-measured hemodynamic variables (i.e., O₂Hb and HHb) that the NIRS modality has some utility as a technology for active brain computer interfaces (e.g., [31–36]). Taken together, these findings suggest the potential of the technique as the measurement basis for an automated cognitive tracking technology. However, to date there have been no studies conducted to evaluate whether or not NIRS signals could be used for robust classification of different levels of attention during tasks requiring sustained attention. The primary object of past NIRS studies on sustained attention focused on better understanding the relationship between NIRS-measured cortical activity and degradation in behavioral performance. The current study aspires to go a step further by investigating the performance of a NIRS-based classification analysis aiming at distinguishing changes in the level of attention.

It is also worth noting that most of the aforementioned NIRS studies focused on one area of interest, the prefrontal cortex (PFC, [23–25,27–30]). The PFC represents an appropriate candidate to investigate attention-related changes in brain activity since it has been described on numerous occasions as a cortical area significantly involved in human cognition (e.g., [37]). There are also convenient, practical benefits to mounting NIRS probes on this scalp area. One such benefit is that compared to other, more dorsal areas, the scalp in this region is hairless. Hair presents a well-known problem in NIRS as it can impact dramatically on both photon absorption and the coupling of the probes with the underlying scalp [38]. The associated optical losses can severely degrade the signal-to-noise ratio reducing the reliable interpretability of the signal. Another important benefit of PFC-oriented measurement is that by focusing on a single specific cortical area, the measurement setup is consistent with the aim of developing practical, ambulatory cognitive-state tracking technologies since it allows for a reduction in the number of measurement channels required at the scalp level. However, by investigating PFC activity only, NIRS studies in the field may miss other relevant information conveyed, potentially, by activity in other task-relevant cortical areas. Excluding information from such areas could limit the potential classification accuracy of NIRS-based classification of cognitive states. It is then crucial to investigate the potential of other attention-related areas' activity, as measured through NIRS, to better capture the attention decrement. Lesion studies in patients [39] as well as neuroimaging studies in healthy subjects [40–42] suggest a significant role for the right parietal area in sustained attention processes and changes in activity under this area has been suggested as involved in attention changes [26,43,44]. This cortical region represents then another potential candidate for the discrimination of changes in the level of attention. Testing this hypothesis is an important aspect of the research described here.

Selecting the most discriminative variable(s)/feature(s) is an important aspect of any machine-learning problem [45]. Given that none of the aforementioned sustained attention studies performed any NIRS-based classification analysis, there are currently no guidelines concerning which NIRS variables to focus on in order to detect as accurately as possible any decrement in the level of attention. While some previous studies demonstrated that the HHb variable was insensitive to time-on-task during a sustained attention task (e.g., [28]), others have described significant changes in both the HHb and O₂Hb variables throughout sustained attention tasks [23,24,46]. In the study described here, we hope to shed light on these discrepancies by

investigating classification performance based on the O₂Hb variable, the HHb variable and a combination of both.

In summary, as part of efforts to develop effective cognitive-state tracking technologies, this paper reports on a study investigating the potential of detecting attention decrements during a sustained attention task through optical measurement of related brain activity. Beyond this primary investigation, we also seek to test the hypotheses that (i) in addition to the PFC, other attention-related areas (i.e., the right parietal area) may facilitate the detection of attention decrement with good accuracy and (ii) exploiting both NIRS variable(s) (i.e., O₂Hb and HHb) is valuable in improving performance for such efforts.

Materials and Methods

Participants

Seven male volunteers took part in this classification study (aged 29.0±6.6 years). All subjects were right-handed according to the Edinburgh Questionnaire [47]. None of the subjects reported that they suffered from neurological, respiratory, and cardiovascular disease or medication, which might affect brain perfusion and function. All procedures were approved by the local Institutional Review Board for the Protection of Human Subjects (CPP Sud-Méditerranée II, number 2010-11-05) and complied with the Declaration of Helsinki for human experimentations. Each subject provided written informed consent prior to participation.

Experimental Set-up

Experiments were conducted in a quiet and dimly lit room. Each subject performed the entire protocol once. The subjects were seated at a table on which a stimulus light (white) source was positioned level with the eyes at a distance of 1 m. The left forearm of each subject was rested upon the surface of the table. The dominant hand (i.e., right hand) was held in a neutral position in the sagittal plane. The angle of the elbow was set to 110° (with 180° corresponding to full elbow extension). The thumb was fixed against a dynamometer allowing direct measurement of abduction force (Captels, Saint-Mathieu-de-Trévières, France).

Experimental Protocol

First, a standard warm-up phase was performed consisting of twenty static submaximal contractions of the right abductor pollicis brevis (i.e., through a thumb abduction task) in an intermittent mode. The level of force was maintained for five seconds followed by five seconds of recovery and was gradually increased after the tenth contraction. Visual feedback of the level of force generated was given in real-time on a computer screen positioned in front of the subjects. Once the warm-up phase was realized, the computer screen was turned off and a simple visual RT task was performed over the course of one minute in order to familiarize the subjects with the paradigm. The task onset signal consisted of a flash (150 ms duration) delivered using the light source (i.e., photodiode arrays consisting of a few dozen emitters). A randomly varying inter-stimuli interval (ISI) was set with a range of between two and fifteen seconds. The motor response requested from the subject was a thumb abduction task to be performed as quickly as possible in response to the visual stimulus. In this sense, the task exploited in our protocol closely replicated the characteristics of the psychomotor vigilance test (PVT) developed by Dinges *et al.* [48]. Such a simple RT task has been shown to be highly sensitive to changes in attention [2,48]. Further, during simple RT tasks, the stimulus saliency remains constant throughout the task and the maintenance of optimal performance is therefore only mediated through top-down processes without any

stimulus-driven increase in the level of attention. Following the familiarization RT task, the subjects were instructed to rest for two minutes in order to produce a reference resting state in the NIRS signals. This was followed by a sustained attention task of thirty minutes whose characteristics were the same as those during the one minute familiarization task. Over the course of the experiment, event labels were set using the NIRS acquisition software (V6.0, Artinis, The Netherlands) in order to demarcate the periods of interest (*i.e.*, baseline and task). Immediately after the experiment, the rating of perceived exertion (RPE) was evaluated by means of the Borg scale (from 6 to 20; [49]). The time course of the experimental protocol is presented in Figure 1.A.

Measurements

Reaction time. The force/motor responses and stimulus signals were synchronized and digitized at 2,048 samples per second using the Biopac MP100 data acquisition system (Biopac System, Inc., Santa Barbara, CA).

Near-Infrared spectroscopy. The NIRS technique has been described elsewhere [13]. NIRS measurements were performed using a continuous wave (CW) multichannel NIRS system (Oxymon Mark III, Artinis, The Netherlands). The data acquisition sampling rate was set to 10 Hz. This system allows measurement of changes in optical density at two different wavelengths in the near-infrared range (nominal wavelengths 763 and 855 nm) before converting these into changes in concentration levels of [O₂Hb] and [HHb]. A subject-specific differential pathlength factor (DPF) was used for this conversion based on the age of each subject [50] and this allowed measurement of the concentration changes of [O₂Hb] and [HHb] in μM [51]. The emitter-detector distance was set to 3.5 cm. In the present study, the measurements were performed using seven channels over the regions of interest. Three were positioned over the frontopolar part of the left, the right and the medial prefrontal cortex (IPFC, rPFC and mPFC, respectively), and four over the right parietal area. The probes were placed according to the modified international EEG 10–10 system [52] and mounted on a custom-made cap fixated by several bands surrounding the head of the subject. According to the EEG 10–10 system, the locations of the centers of the channels over the IPFC, rPFC and mPFC corresponded to the Fp1, Fp2 and Fpz points, respectively. The centers of the 4 channels set in a square template over the right parietal area corresponded to the P6 point. A representation of the channel locations can be seen in Figure 2. During the probe placement, the Oxysoft software (V6.0, Artinis, The Netherlands) allowed real time assessment of the quality of the NIRS signals for each of the seven channels based on the light source power level and the receiver gain. Once an acceptable signal-to-noise ratio was obtained according to the signal quality assessment, a zero baseline was set and the protocol was executed.

Data Analyses

Behavioral data. The RT data was processed through the Acknowledge software associated with the Biopac system (Acknowledge 3.8.1, Biopac Systems, Santa Barbara, CA, USA). The RT was measured as the time between the flash stimulus (target stimulus) and the beginning of force production. Responses were considered correct if the dynamometer was engaged between 150 and 600 ms after stimulus onset. All other responses were considered incorrect. Such a cut-off time window has been exploited in other RT studies (*e.g.*, [53]) and facilitates the exclusion of outlying RT values in the dataset. We calculated RTs of the first ten and last ten minutes of the task and then computed averages of the RTs obtained for these two periods.

Near-Infrared spectroscopy. Signal preprocessing: The oxy- and deoxy-hemoglobin signals acquired from the NIRS instrumentation were initially filtered using a fourth order digital low-pass Butterworth filter with a cut-off frequency of 0.1 Hz in order to remove the heart rate and respiratory components [54]. Next, movement artifacts were removed on specific, visually identified channels by using moving standard deviation and spline interpolation routines in Matlab (Mathworks, Natick, MA). This method has been validated using simulated, as well as real NIRS signals and has been shown to improve the detection of evoked hemodynamic responses (see [55], for details). Finally, given that the datasets contained information regarding cortical hemodynamic changes over several regions of the brains and from many different subjects, a z-normalization of the signals was performed. From the resulting signals, a supervised classification procedure was performed by means of a linear support vector machine (SVM) algorithm.

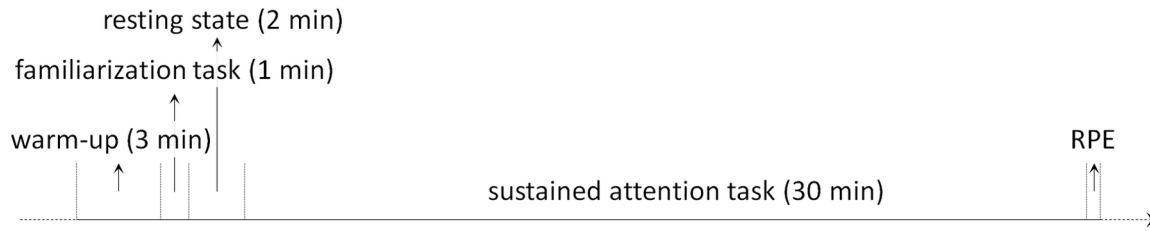
NIRS data classification using support vector machines: SVM can be considered as one of the most powerful classification algorithms as it is able to learn linear decision boundaries as well as more complex ones with relatively low complexity and few user-defined hyper parameters [56]. Nonlinear decision boundaries are learned using the “kernel-trick” which consists of mapping the data into a higher-dimensional space using a kernel function and finding a linear separation in that space. An example of kernel function is the Radial Basis Function (RBF) defined as follows:

$$K(x,y) = \exp\left(-\frac{\|x-y\|^2}{2\sigma^2}\right)$$

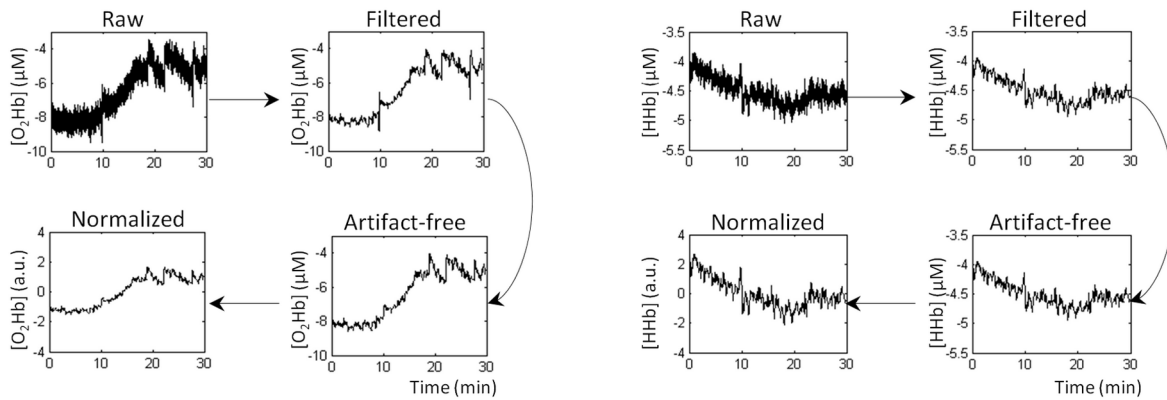
Where x and y are two data points and σ is the width of the RBF.

In the current study, we used a linear SVM (*i.e.*, using linear kernel) as the decision boundary between the two brain states (*i.e.*, full attention vs. attention decrement) appeared to be sufficiently linear. The linear SVM has already been used in previous studies on attention decrement detection based on EEG signals, illustrating high classification accuracy results (*e.g.*, [7]). Like other linear classifiers (*e.g.*, linear discriminant analysis, LDA), a linear SVM uses a hyperplane to separate data points from each class. Additionally, the linear SVM chooses the hyperplane with the maximal distance from the nearest training points. This distance is called the “margin” and the nearest training points to the optimal hyperplane are called “support vectors”. Figure 1.C. shows an illustrative example of an optimal hyper-plane as constructed by a linear SVM. Margin maximization increases generalization ability of the classification algorithm. However, such a learning scheme is sensitive to outliers and overtraining. For this reason, a regularization parameter C is used to reduce data over-fitting. Depending on C , the optimal margin will either expand or diminish and more or less points will subsequently become support vectors, respectively [56,57]. In the current study, we used the default value of 1 for the regularization parameter C with the software Weka (version 3.6.8, University of Waikato Hamilton, New Zealand). We designed the SVM for two-class classification (*i.e.*, full attention versus attention decrement). The NIRS signals from the first ten minutes of the task were considered as characterizing the ‘full attention’ class, while the NIRS signals from the last ten minutes of the task were considered as characterizing the ‘attention decrement’ class (this assumption was then supported by analyzing the RT values as described below; see RT results, Figure 3). Classification analyses were performed over data segmented and averaged over one second duration epochs.

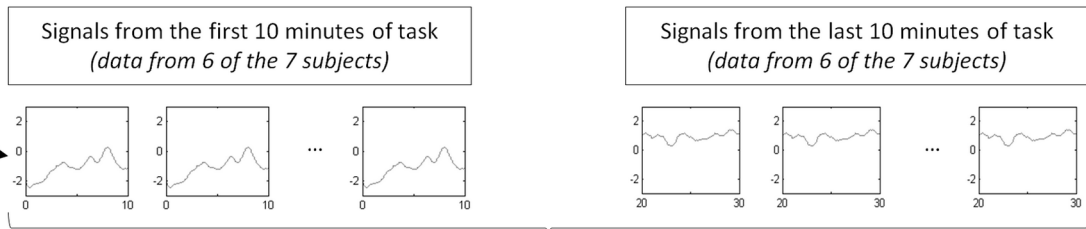
A. Experimental protocol



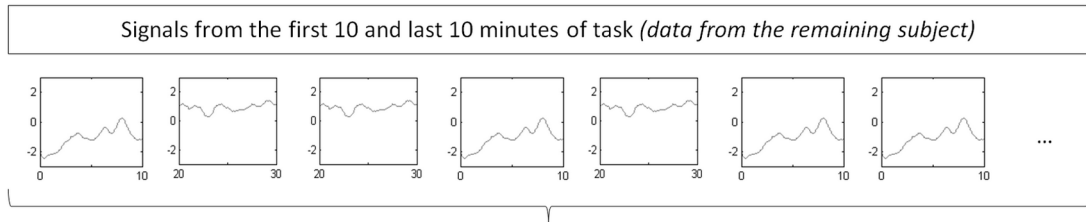
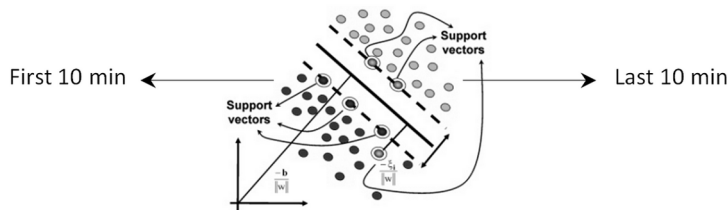
B. NIRS signals preprocessing



C. Pattern classification (SVM)



SVM training



SVM test

Calculation of % of correctly classified epochs

Figure 1. Illustration of the experimental protocol and analysis procedure. A. Time course of the experimental protocol. RPE: Rate of Perceived Exertion. **B. NIRS signals preprocessing steps.** *Left:* O₂Hb signals. *Right:* HHb signals. **C. NIRS signals classification based on SVM.** *From top to bottom:* Filtered, artifact-free, normalized signals are first exploited in the SVM learning step using six of the seven subjects. A model is built, represented here by its feature space. Finally, a SVM test is performed using the signals of the single remaining subject and the percentage of correctly classified epochs is computed. See Methods for further details. doi:10.1371/journal.pone.0092045.g001

Thus, for each subject, six hundred time points were obtained for each class (i.e., sixty seconds \times ten minutes) and constituted the corresponding point clouds within the feature space. The signal feature selected was the magnitude (i.e., averaged for each one second duration epoch) of concentration values (in μM) of the considered NIRS variable(s): [O₂Hb], [HHb] or both [O₂Hb] and [HHb]. Also, classification was based on the NIRS signals from (i) the PFC area exclusively, (ii) the right parietal area exclusively and (iii) both the PFC and the right parietal areas. These distinct feature vectors allowed us to investigate classification accuracy over a range of NIRS variables and cortical area(s). By doing so, the resultant feature pool was comprised of between three (i.e., using [O₂Hb] or [HHb] from the three channels over the PFC) and fourteen features (i.e., using both [O₂Hb] and [HHb] from the seven recorded channels). Data obtained from six of the seven subjects were exploited as the training set. Once the training step was realized, each class of the resulting feature space consisted of three thousand six hundred points (i.e., six hundred points \times six subjects). The test data set consisted of the data of the remaining subject. This process of leave-one-out cross-validation was repeated to assess the classification accuracy across all subjects. Classification accuracy was calculated as the percentage of correctly classified epochs for each part of the data (i.e., first or last minutes of task). All of the processing steps are presented in Figure 1.

Statistical Analysis

Statistica software (version 7.0, Statsoft, Oklahoma, United-States) was used for all analyses. All data were examined for normality using skewness and kurtosis tests. The Student t-test was used to test for any significant effect of time (i.e., first ten versus last ten minutes of the task) on the changes in RT. Effect size was calculated on the RT values using Cohen's effect size d (d effects: small ≥ 0.2 , medium ≥ 0.5 , large ≥ 0.8), defined as the mean change score divided by the standard deviation of change [57]. The significance level was set at $p < .05$. Data are presented as mean \pm standard deviation (SD).

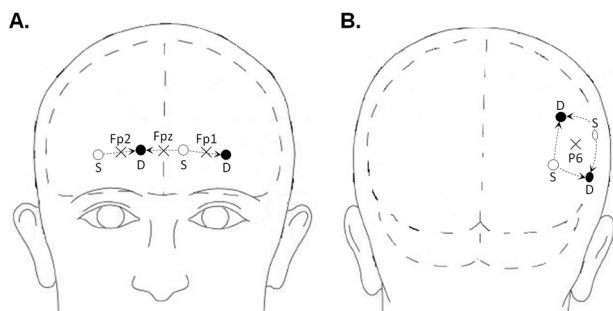


Figure 2. Placement of NIRS probes. Frontal (A) and dorsal (B) views are represented. Crosses represent locations from the EEG 10-10 system. Empty circles - noted "S" - represent sources and black circles - noted "D" - represent detector probes. doi:10.1371/journal.pone.0092045.g002

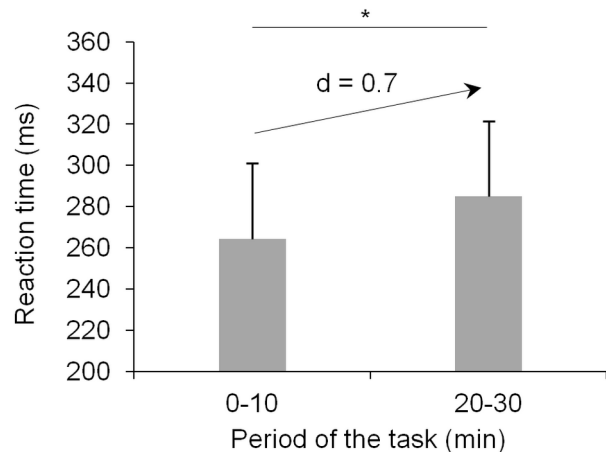


Figure 3. Changes in mean reaction time from the first ten to the last ten minutes of the task. A significant increase in RT occurred at the end (last ten minutes) compared to the beginning (first ten minutes) of the task. Cohen's effect size d value for this difference is specified above the centered arrow. * $p < .05$. Vertical bars represent SD. doi:10.1371/journal.pone.0092045.g003

Results

Behavioral Results

As expected, the RT results demonstrated that attention decrement occurred towards the end of the task. The Student t-test demonstrated that RT values were significantly higher in the last ten than for the first ten minutes of the task ($t_6 = 3.1$; $p < .05$). The Cohen's effect size d value for this difference was 0.7, corresponding to a medium-to-large effect. These results are presented in Figure 3. The RPE score after the experiment was 14.9 ± 1.7 , a value corresponding to "hard" according to the scale.


Classification Accuracy

All the classification accuracy results, including analyses exploiting [O₂Hb], [HHb] and both [O₂Hb] and [HHb] as features of interest from the PFC area exclusively, the right parietal area exclusively and both the PFC and the right parietal areas, are presented in Figure 4. The main results indicate that (i) the highest classification accuracy results were obtained when exploiting the oxyhemoglobin signals (i.e., from 77 to 89%, depending on the cortical area considered) rather than the deoxyhemoglobin signals (i.e., from 65 to 66%) and (ii) the classification accuracy was increased to about 90% when using signals from the right parietal area rather than from the prefrontal cortex.

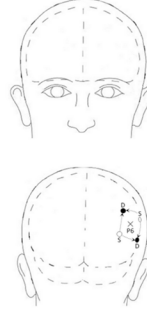
Discussion

This study aimed to investigate the potential of harnessing NIRS-measured cortical activity for the detection of time-on-task related changes in the level of attention during a sustained

A.			
Subject	[O ₂ Hb]	[HHb]	[O ₂ Hb] and [HHb]
1	44.5	87.8	88.8
2	73.5	94.2	89.1
3	49.2	28.4	32.1
4	95.1	90.4	90.6
5	98.4	80.6	76.5
6	82.5	21.2	68.3
7	100	60.8	96.7
Mean ± SD	77.6 ± 23	66.2 ± 30.3	77.4 ± 22.2



B.			
Subject	[O ₂ Hb]	[HHb]	[O ₂ Hb] and [HHb]
1	94.9	94	99.6
2	85.4	81.6	97.9
3	91.7	22.6	77
4	100	26.4	91.3
5	83.8	45	72.2
6	76.3	86.1	100
7	96.4	100	97.2
Mean ± SD	89.8 ± 8.3	65.1 ± 32.8	90.7 ± 11.5



C.			
Subject	[O ₂ Hb]	[HHb]	[O ₂ Hb] and [HHb]
1	60.8	100	91.8
2	85	96.5	96.3
3	39.8	6.6	34.2
4	92	34.5	96.7
5	94	61.4	74.7
6	75.5	70.7	93.9
7	92.2	93.9	96.8
Mean ± SD	77 ± 20.2	66.2 ± 35.1	83.5 ± 23.1

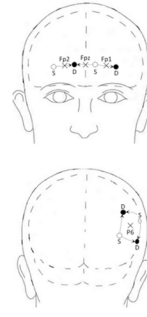


Figure 4. Detailed classification accuracy results. The classification accuracy results using NIRS signals from the prefrontal (A), the right parietal (B) and both the prefrontal and the right parietal areas (C) are provided. From left to right, the columns present (i) subject number, the classification accuracy - in percentage of total classification trials - exploiting (ii) [O₂Hb], (iii) [HHb] and (iv) both [O₂Hb] and [HHb] as features of interest. doi:10.1371/journal.pone.0092045.g004

attention task. Our experimental design produced a decrement in the level of attention as revealed by the significant increase in RT in the last ten compared to the first ten minutes of the task ($p < .05$; $d = 0.7$). The results demonstrate that relatively good classification accuracy can be obtained using NIRS variables (O₂Hb and/or HHb) to detect the changes in the attentional state observed at the behavioral level. It is worth noting that the classification accuracy was lowest when exploiting the HHb signals only (i.e., from 65 to 67% in average), regardless of the cortical area considered.

Moreover, the classification accuracy was increased to about 90% when using signals from the right parietal area. These findings are examined in detail next.

Methodological Considerations and Study Limitations

As already mentioned, the task studied here closely replicated the characteristics of the psychomotor vigilance test (PVT) developed by Dinges *et al.* [48] and an increase in RT has been previously demonstrated for such a PVT, even for a task of twenty

minutes duration [2]. As expected, a significant increase in RT occurred during this simple RT task of thirty minutes duration. In addition to the longer RT, relatively high RPE values were reported by the subjects (i.e., 14.9 ± 1.7 on a scale ranging from 6 to 20), which demonstrates the cognitive loading (sustaining of attention) demanded with such a simple sustained attention task [58]. Also, Lim *et al.* [2] have shown that the increase in RT observed during their simple RT task of twenty minutes duration was accompanied by high subjective fatigue ratings after the task - subjective fatigue being well-known to affect sustained attention abilities [59]. Taken together, these results support the conclusion that the task exploited in the current study induced a time-on-task related attention decrement.

As discussed by Shen *et al.* [7], one weakness of past studies exploiting EEG to detect attention decrement was the lack of subject-wise cross-validation in their performance evaluation (e.g., [60]). We therefore applied, as in [7], a “leave-one-out” scheme (which is a conventional approach to evaluate the performance of machine learning methods for small data sets) in order to evaluate the subject-independent accuracy performance. Using this leave-one-out cross-validation procedure, high classification accuracy was confirmed with up to 90% scores achieved in classifying attention state based on NIRS signals. The use of such a cross-validation procedure was particularly appropriate in this study as we had a relatively small number of subjects ($n = 7$), a small sample size which may be considered a study limitation. It is worth adding the caveat that leave-one-out schemes may induce, for small sample sizes, a bias in the error estimation [61]. Using a larger number of subjects would facilitate the exploitation of other validation schemes such as *k*-fold cross-validation which may afford less biased estimations of the model generalization error.

Another potential issue in the current study was the lack of control for any skin flow contributions to the NIRS signals and again, this may be regarded as a study limitation. Recent studies have raised the issue of superficial - extra-cortical - contributions in NIRS signals, specifically in the O_2Hb signal [62]. The analysis of the photon time-of-flight distribution in time-domain NIRS [63,64] or the use of additional short emitter-detector separation as regressors [65,66] have been proposed as methods to separate cortical and extracortical contributions in NIRS signals. In the study described here, the clear variability in attention decrement-sensitivity across the cortical areas investigated does not support the idea of a global systemic response biasing the feature space. The observed increased activity from areas known to be involved in attention suggest that the features identified reflect localized cortical vascular dynamics. The use of the aforementioned methods would have however helped identify the precise nature of the contribution from cortical components in the optical signals obtained.

The regional variation in the differential path-length factor (DPF) identified in the literature [67] might also have affected the measured regional changes in NIRS signals. We exploited a subject-specific DPF based on the age of each subject as proposed by Duncan *et al.* [50] and this allowed the measurement to be converted into changes in concentration levels of $[O_2Hb]$ and $[HHb]$. In order to eliminate the heterogeneous effect of regional DPF variations across the full extent of the measurement area, the signals were normalized through expression in terms of percentage changes (Figure 1.B.). Future NIRS investigation might however implement region-specific DPF in addition to subject-specific DPF.

Finally, our classification procedure specifically aimed at classifying attention decrement-related lapses in attention, as they occur during time-on-task activities. To do so, we exploited the first and last ten minutes of the task to label our classes. An

alternative means to detect changes in the level of attention could involve labeling the brain states of interest using moment-to-moment variations in behavioral performance (e.g., RT). Doing so would facilitate the detection of changes in the level of attention on shorter time scales, as they occur momentarily, but such an approach is beyond the scope of the current study.

Region of Interest: Right Parietal Area Versus PFC

This study aimed, in part, at testing the appropriateness of focusing on the PFC to detect decrements in the level of attention. The emphasis on the PFC which has characterized research to date in this field [23–25,27–30] has probably been as a consequence of an *a priori* knowledge-driven choice (i.e., the PFC area has been identified as involved in a large number of cognitive functioning studies) and because of technical advantages that presents this hairless scalp area conveniently for NIRS investigation. In contrast, our experimental investigation has taken a data-driven approach to deduce which of the attention-related cortical areas offers the best classification accuracy when investigated using NIRS. We hypothesized that, given its implication in sustained attention tasks, the right parietal area would represent another potentially relevant candidate area over which to discriminate changes in the level of attention.

For both analyses, based on the PFC or on the right parietal area signals, relatively good classification results were obtained, however performance was on average much better when exploiting NIRS signals recorded over the right parietal area (see Figure 4.B). This finding is not surprising when one considers the aforementioned, crucial role of this area in sustained attention tasks [39–42]. This result raises design dilemmas for NIRS-based cognitive-state tracking technology: would it be preferable to focus on the right parietal area – which yields better discrimination and reduces then the possibility of false positives in the detection of attention decrement? Or rather, would it be better to continue to focus on the PFC which offers undeniable technical advantages for NIRS investigation, but offers poorer sensitivity to attention decrement? Although the presence of hair over the parietal area did not impact the classification accuracy results of our study, it was technically more complex, and hence took more time to set up than when measuring over the PFC. The problem of obtaining qualitatively good NIRS signals over hair-covered scalp areas is well-known from NIRS investigators and has been identified as an issue in motor area-based brain-computer interface design [16]. The challenge for future NIRS technological developments is to provide a NIRS optode mounting system which can resolve this problem of hair-related photon absorption. In such conditions, focusing on the right parietal area for detecting attention decrement in a real world context could become more convenient. It is worth commenting too that the positioning of probes over the parietal cortices is likely to be much more acceptable to users given that it is aesthetically less intrusive than the alternative which would require the mounting of a set of optodes and sensing technology on the face (i.e., the forehead).

Finally, it is worth commenting on the finding that combining signals from both the PFC and the right parietal areas did not improve classification performance accuracy over the use of features from the right parietal area only in our classification analyses. This result potentially indicates that, rather than being additive or even multiplicative, information extracted from neural signatures of attention decrement over the PFC and right parietal areas may be redundant. In the purpose of developing practical, ambulatory cognitive-state tracking technologies, we previously mentioned that the number of measurement channels required at the scalp level should be minimized. Thus, the right parietal area

may, on its own, represent an appropriate measurement area for NIRS-based detection of attention decrement.

Variable of Interest: O₂Hb versus HHb

The second objective of this study was to determine which NIRS variable(s) should be exploited for the purpose of distinguishing changes in the level of attention. As mentioned in the introduction, some authors failed to find any changes in HHb in response to time-on-task, even during a sustained attention task of 3 hours duration [28]. The classification results here support the results of Li *et al.* [28], and provide further evidence that the HHb variable has poor sensitivity to time-on-task related changes in the level of attention. This result can be explained by the existence of smaller changes in HHb compared to that in O₂Hb during neurovascular coupling - a phenomenon well “represented” by the balloon model [68]. Also, changes in O₂Hb have been described to more directly reflect cortical activation than HHb due to its superior contrast-to-noise ratio [69], and previous NIRS studies have even proposed that researchers should focus on O₂Hb - rather than HHb - as the variable of interest to determine changes in cortical activity [26,70].

The combination of both O₂Hb and HHb variables in our classification analysis, in some cases improves performance. This increase is minor when measured over the right parietal area (about 1%) and the combination of variables in that example is of minimal utility. As one problem in developing useful cognitive-state tracking technologies is that of reducing its computational requirements [6] here again, a choice has to be made between two alternatives, that is: either (i) exploiting both the O₂Hb and the HHb variables as features of interest in order to marginally improve performance at the cost of increased computational overhead (i.e., by doubling the dimension of the feature space) or (ii) focusing on the O₂Hb to reduce the computational cost with a

minor loss in classification performance. In our opinion, the latter alternative appears to be the more appropriate choice for the purpose of future real-time applications although it depends on the precise use-case envisaged.

Conclusion and Perspectives

To the best of our knowledge, the present study is the first to describe an approach to detect changes in the level of attention through monitoring hemodynamic signals and the results may serve as a further step towards the development of a NIRS-based cognitive state tracking system. Our data-driven approach leads to the conclusion that (i) the right parietal area represents a better choice for the positioning of optodes as it is less intrusive and more sensitive than the PFC and (ii) the O₂Hb variable appears to be sufficiently sensitive for characterization of attention decrements as they occur in cortical areas. The results also demonstrate that optical neuroimaging constitutes a relevant method of significant potential for cognitive state monitoring. We feel the method may have most benefit through integration within a hybrid system context where a combination of complementary modalities (e.g., EEG and NIRS) may provide more robust performance over each modality used in isolation.

Acknowledgments

The authors would like to thank the engineer Jean-Paul MICALLEF for the development of experimental materials.

Author Contributions

Conceived and designed the experiments: Gérard Derosière SP TW. Performed the experiments: Gérard Derosière. Analyzed the data: Gérard Derosière SD Gérard Dray. Wrote the paper: Gérard Derosière SD SP Gérard Dray TW.

References

- Weissman DH, Roberts KC, Visscher KM, Woldorff MG (2006) The neural bases of momentary lapses in attention. *Nat Neurosci* 9: 971–978.
- Lim J, Wu WC, Wang J, Detre JA, Dinges DF, et al. (2010) Imaging brain fatigue from sustained mental workload: an ASL perfusion study of the time-on-task effect. *Neuroimage* 49: 3426–3435.
- Czeisler CA, Walsh JK, Roth T, Hughes RJ, Wright KP, et al. (2005) Modafinil for excessive sleepiness associated with shift-work sleep disorder. *N Engl J Med* 353: 476–486.
- Grandjean E (1979) Fatigue in industry. *British Journal of Industrial Medicine* 36: 175–186.
- Lal SK, Craig A (2001) A critical review of the psychophysiology of driver fatigue. *Biol Psychol* 55: 173–194.
- Johnson RR, Popovic DP, Olmstead RE, Stikic M, Levendowski DJ, et al. (2011) Drowsiness/alertness algorithm development and validation using synchronized EEG and cognitive performance to individualize a generalized model. *Biol Psychol* 87: 241–250.
- Shen KQ, Li XP, Ong CJ, Shao SY, Wilder-Smith EP (2008) EEG-based mental fatigue measurement using multi-class support vector machines with confidence estimate. *Clin Neurophysiol* 119: 1524–1533.
- Caffier PP, Erdmann U, Ullsperger P (2003) Experimental evaluation of eye-blink parameters as a drowsiness measure. *Eur J Appl Physiol* 89: 319–325.
- Seegerstrom SC, Nes LS (2007) Heart rate variability reflects self-regulatory strength, effort, and fatigue. *Psychol Sci* 18: 275–281.
- Dong Y, Hu Z, Uchimura K, Murayama N (2011) Driver inattention monitoring system for intelligent vehicles: A review. *Intelligent Transportation Systems, IEEE Transactions on* 12: 596–614.
- Yang G, Lin Y, Bhattacharya P (2010) A driver fatigue recognition model based on information fusion and dynamic Bayesian network. *Information Sciences* 180: 1942–1954.
- Ferrari M, Quaresima V (2012) A brief review on the history of human functional near-infrared spectroscopy (fNIRS) development and fields of application. *Neuroimage* 63: 921–935.
- Perrey S (2008) Non-invasive NIR spectroscopy of human brain function during exercise. *Methods* 45: 289–299.
- Ayaz H, Shewokis PA, Bunce S, Izzetoglu K, Willems B, et al. (2012) Optical brain monitoring for operator training and mental workload assessment. *Neuroimage* 59: 36–47.
- Bunce SC, Izzetoglu M, Izzetoglu K, Onaral B, Pourrezaei K (2006) Functional near-infrared spectroscopy. *IEEE Eng Med Biol Mag* 25: 54–62.
- Coyle SM, Ward TE, Markham CM (2007) Brain-computer interface using a simplified functional near-infrared spectroscopy system. *J Neural Eng* 4: 219–226.
- Izzetoglu K, Bunce S, Izzetoglu M, Onaral B, Pourrezaei K (2004) Functional near-infrared neuroimaging. *Conf Proc IEEE Eng Med Biol Soc* 7: 5333–5336.
- Strangman G, Boas DA, Sutton JP (2002) Non-invasive neuroimaging using near-infrared light. *Biol Psychiatry* 52: 679–693.
- Villringer A, Chance B (1997) Non-invasive optical spectroscopy and imaging of human brain function. *Trends Neurosci* 20: 435–442.
- Derosiere G, Mandrick K, Dray G, Ward TE, Perrey S (2013) NIRS-measured prefrontal cortex activity in neuroergonomics: strengths and weaknesses. *Front. Hum. Neurosci.* 7: 583. doi: 10.3389/fnhum.2013.00583.
- Parasuraman R (2013) Neuroergonomics: Brain-inspired Cognitive Engineering in Lee JD, Kirlik A, editors. *The Oxford Handbook of Cognitive Engineering*. pp159–177.
- Villringer A, Dirnagl U (1995) Coupling of brain activity and cerebral blood flow: basis of functional neuroimaging. *Cerebrovasc Brain Metab Rev* 7: 240–276.
- Butti M, Pastori A, Merzagora A, Bianchi A, Bardoni A, et al. (2006) Combining near infrared spectroscopy and functional MRI during continuous performance test in healthy subjects. *Conf Proc IEEE Eng Med Biol Soc* 1: 1944–1947.
- Butti M, Pastori A, Merzagora A, Zucca C, Bianchi A, et al. (2006) Multimodal analysis of a sustained attention protocol: continuous performance test assessed with near infrared spectroscopy and EEG. *Conf Proc IEEE Eng Med Biol Soc* 1: 1040–1043.
- De Joux N, Russell PN, Helton WS (2013) A functional near-infrared spectroscopy study of sustained attention to local and global target features. *Brain Cogn* 81: 370–375.
- Derosiere G, Billot M, Ward ET, Perrey S (2013) Adaptations of Motor Neural Structures' Activity to Lapses in Attention. *Cereb Cortex*. doi: 10.1093/cercor/bht206.
- Helton WS, Hollander TD, Warm JS, Tripp LD, Parsons K, et al. (2007) The abbreviated vigilance task and cerebral hemodynamics. *J Clin Exp Neuropsychol* 29: 545–552.

28. Li Z, Zhang M, Zhang X, Dai S, Yu X, et al. (2009) Assessment of cerebral oxygenation during prolonged simulated driving using near infrared spectroscopy: its implications for fatigue development. *Eur J Appl Physiol* 107: 281–287.
29. Shaw TH, Funke ME, Dillard M, Funke GJ, Warm JS, et al. (2013) Event-related cerebral hemodynamics reveal target-specific resource allocation for both “go” and “no-go” response-based vigilance tasks. *Brain Cogn* 82: 265–273.
30. Warm JS, Parasuraman R, Matthews G (2008) Vigilance requires hard mental work and is stressful. *Hum Factors* 50: 433–441.
31. Power SD, Kushki A, Chau T (2012) Intersession Consistency of Single-Trial Classification of the Prefrontal Response to Mental Arithmetic and the No-Control State by NIRS. *PLoS ONE* 7(7): e37791.
32. Nambu I, Ebisawa M, Kogure M, Yano S, Hokari H, et al. (2013) Estimating the Intended Sound Direction of the User: Toward an Auditory Brain-Computer Interface Using Out-of-Head Sound Localization. *PLoS ONE* 8(2): e57174.
33. Cui X, Bray S, Reiss AL (2010) Speeded Near Infrared Spectroscopy (NIRS) Response Detection. *PLoS ONE* 5(11): e15474.
34. Sitaram R, Zhang H, Guan C, Thulasidas M, Hoshi Y, et al. (2007) Temporal classification of multichannel near-infrared spectroscopy signals of motor imagery for developing a brain–computer interface. *NeuroImage* 34: 1416–1427.
35. Naseer N, Hong MJ, Hong KS (2013) Online binary decision decoding using functional near-infrared spectroscopy for development of a brain-computer interface. *Exp Brain Res* doi: <http://dx.doi.org/10.1007/s00221-013-3764-1>.
36. Naseer N, Hong KS (2013) Classification of functional near-infrared spectroscopy signals corresponding to right- and left-wrist motor imagery for development of a brain-computer interface. *Neuroscience Letters* 553: 84–89.
37. Koechlin E, Basso G, Pietrini P, Panzer S, Grafman J (1999) The role of the anterior prefrontal cortex in human cognition. *Nature* 399: 148–151.
38. Murkin JM, Arango M (2009) Near-infrared spectroscopy as an index of brain and tissue oxygenation. *Br J Anaesth* 103 Suppl 1: i3–13.
39. Posner MI, Rafal RD (1987) Cognitive theories of attention and the rehabilitation of attentional deficits. In Meier MJ, Benton AL, Diller L, editors. *Neuropsychological Rehabilitation*. 182–201.
40. Coull JT (1998) Neural correlates of attention and arousal: insights from electrophysiology, functional neuroimaging and psychopharmacology. *Prog Neurobiol* 55: 343–361.
41. Fink GR, Halligan PW, Marshall JC, Frith CD, Frackowiak RS, et al. (1997) Neural mechanisms involved in the processing of global and local aspects of hierarchically organized visual stimuli. *Brain* 120 (Pt 10): 1779–1791.
42. Pardo JV, Fox PT, Raichle ME (1991) Localization of a human system for sustained attention by positron emission tomography. *Nature* 349: 61–64.
43. Coull JT, Frackowiak RS, Frith CD (1998) Monitoring for target objects: activation of right frontal and parietal cortices with increasing time on task. *Neuropsychologia* 36: 1325–1334.
44. Paus T, Zatorre RJ, Hofle N, Caramanos Z, Gotman J, et al. (1997) Time-related changes in neural systems underlying attention and arousal during the performance of an auditory vigilance task. *J Cogn Neurosci* 9: 392–408.
45. Shen KQ, Ong CJ, Li XP, Wilder-Smith EP (2008) Feature selection via sensitivity analysis of SVM probabilistic outputs. *Machine Learning* 70: 1–20.
46. Fallgatter AJ, Strik WK (1997) Right frontal activation during the continuous performance test assessed with near-infrared spectroscopy in healthy subjects. *Neurosci Lett* 223: 89–92.
47. Oldfield RC (1971) The assessment and analysis of handedness: the Edinburgh inventory. *Neuropsychologia* 9: 97–113.
48. Dinges DF, Pack F, Williams K, Gillen KA, Powell JW, et al. (1997) Cumulative sleepiness, mood disturbance, and psychomotor vigilance performance decrements during a week of sleep restricted to 4–5 hours per night. *Sleep* 20: 267–277.
49. Borg G (1970) Perceived exertion as an indicator of somatic stress. *Scand J Rehabil Med*. 2: 92–98.
50. Duncan A, Meek JH, Clemence M, Elwell CE, Fallon P, et al. (1996) Measurement of cranial optical path length as a function of age using phase resolved near infrared spectroscopy. *Pediatr Res* 39: 889–894.
51. Delpy DT, Cope M, van der Zee P, Arridge S, Wray S, et al. (1988) Estimation of optical pathlength through tissue from direct time of flight measurement. *Phys Med Biol* 33: 1433–1442.
52. American Electroencephalographic Society (1994) American Electroencephalographic Society. Guideline thirteen: Guidelines for standard electrode position nomenclature. *J Clin Neurophysiol* 11: 111–113.
53. Faber LG, Maurits NM, Lorist MM (2012) Mental fatigue affects visual selective attention. *PLoS One* 7: e48073.
54. Huppert TJ, Diamond SG, Franceschini MA, Boas DA (2009) HomER: a review of time-series analysis methods for near-infrared spectroscopy of the brain. *Appl Opt* 48: D280–298.
55. Scholkmann F, Spiechtig S, Muehlemann T, Wolf M (2010). How to detect and reduce movement artifacts in near-infrared imaging using moving standard deviation and spline interpolation? *Physiol Meas*, 31: 649–662.
56. Burges CJC (1998) A Tutorial on Support Vector Machines for Pattern Recognition. *Data Mining and Knowledge Discovery* 2: 121–167.
57. Cortes C, Vapnik V (1995). Support-Vector Networks. *Machine Learning* 20: 273–297.
58. Langner R, Eickhoff SB (2012) Sustaining attention to simple tasks: a meta-analytic review of the neural mechanisms of vigilant attention. *Psychol Bull* 139: 870–900.
59. Boksem MA, Meijman TF, Lorist MM (2005) Effects of mental fatigue on attention: an ERP study. *Brain Res Cogn Brain Res* 25: 107–116.
60. Lal SK, Craig A, Boord P, Kirkup L, Nguyen H (2003) Development of an algorithm for an EEG-based driver fatigue countermeasure. *J Safety Res* 34: 321–328.
61. Beleites C, Baumgartner R, Bowman C, Somorjai R, <http://www.sciencedirect.com/science/article/pii/S0169743905000687> - aff2Steiner G, et al. (2005) Variance reduction in estimating classification error using sparse datasets. *Chemometr Intell Lab Syst* 79: 91–100.
62. Kirilina E, Jelzow A, Heine A, Niessing M, Wabnitz H, et al. (2012) The physiological origin of task-evoked systemic artefacts in functional near infrared spectroscopy. *Neuroimage* 61: 70–81.
63. Aletti F, Re R, Pace V, Contini D, Molteni E, et al. (2012) Deep and surface hemodynamic signal from functional time resolved transcranial near infrared spectroscopy compared to skin flow motion. *Comput Biol Med* 42: 282–289.
64. Re R, Muthalib M, Zucchelli L, Perrey S, Contini D, et al. (2013) Multichannel time domain fNIRS mapping of cortical activation and superficial systemic responses during neuromuscular electrical stimulation. In: *European Conferences on Biomedical Optics. International Society for Optics and Photonics*. 880404–880404. <http://dx.doi.org/10.1117/12.2032512>.
65. Gagnon L, Cooper RJ, Yücel MA, Perdue KL, Greve DN, et al. (2012) Short separation channel location impacts the performance of short channel regression in NIRS. *Neuroimage* 59: 2518–2528.
66. Saager RB, Telleri NL, Berger AJ (2011) Two-detector corrected near infrared spectroscopy (C-NIRS) detects hemodynamic activation responses more robustly than single detector NIRS. *Neuroimage* 55: 1679–1685.
67. Hoshi Y (2005) Functional near-infrared spectroscopy: potential and limitations in neuroimaging studies. *Int Rev Neurobiol* 66: 237–266.
68. Buxton RB, Frank LR (1997) A model for the coupling between cerebral blood flow and oxygen metabolism during neural stimulation. *J Cereb Blood Flow Metab* 17: 64–72.
69. Strangman G, Culver JP, Thompson JH, Boas DA (2002) A quantitative comparison of simultaneous BOLD fMRI and NIRS recordings during functional brain activation. *Neuroimage* 17: 719–731.
70. Yamanaka K, Yamagata B, Tomioka H, Kawasaki S, Mimura M (2010) Transcranial magnetic stimulation of the parietal cortex facilitates spatial working memory: near-infrared spectroscopy study. *Cereb Cortex* 20: 1037–1045.